AIAA 80-0685R

Bending of Thick Rectangular Plates Laminated of Bimodulus Composite Materials

C. W. Bert,* J. N. Reddy,† V. Sudhakar Reddy,‡ and W. C. Chao§
University of Oklahoma, Norman, Okla.

A mixed finite-element analysis is presented for static behavior of rectangular plates laminated of composite materials having finite transverse shear moduli and different elastic properties depending upon whether the fiber-direction strains are tensile or compressive. As a benchmark to assess the validity and accuracy of the finite-element analysis, a closed-form solution is given for a two-layer, cross-ply plate having all edges simply supported without in-plane restraint and subjected to sinusoidally distributed normal pressure. Numerical results obtained by the two methods are compared and found to agree quite well.

Nomenclature

A, A_{ij} = stretching stiffnesses for transversely isotropic and cross-ply plates
a, b = plate dimensions in x and y directions
B, B_{ij} = bending-stretching coupling stiffnesses for transversely isotropic and cross-ply plates
C_{rs} = coefficients defined in Eqs. (15)
D, D_{ij} = bending stiffnesses for transversely isotropic and cross-ply plates
d_x = $\partial(\ )/\partial x$
E_c, E_t = compressive and tensile Young's moduli for transversely isotropic bimodulus material
E_f, E_m = fiber and matrix Young's moduli
E_1, E_2, E_3 = Young's moduli in directions x,y,z
F_i^α = generalized force components defined in Eqs. (20)
G_{13}, G_{23} = longitudinal-thickness and transverse-thickness shear moduli of orthotropic material
G_{zc}, G_{zt} = thickness-shear moduli for transversely isotropic bimodulus material
h = total thickness of plate
K = shear-correction coefficient for transversely isotropic plate
K_4, K_5 = shear-correction coefficients for cross-ply plate
K_{ij} = matrix coefficients defined in Eqs. (20)
L_{rs} = linear differential operators defined in Eqs. (8)
M_i, N_i = stress couples and in-plane stress resultants
$\mathfrak{N}_i$ = interpolation function at node i
n = number of nodes per element
Q_c, Q_t = compressive and tensile plane-stress reduced stiffnesses for transversely isotropic bimodulus material
Q_x, Q_y = thickness-shear stress resultants
$\bar{Q}, \Delta Q$ = $\frac{1}{2}(Q_c + Q_t)$, $Q_c - Q_t$
Q_{ijkl} = plane-stress reduced stiffnesses for orthotropic bimodulus material
q, q_0 = normal pressure and its peak value
S, S_{ij} = thickness-shear stiffnesses for transversely isotropic and cross-ply plates
$\mathcal{S}_{ij}$ = matrix coefficients defined in Eqs. (20)
U, V, W = midplane displacement coefficients (amplitudes of u^0, v^0, w^0)
u, v, w = displacements in x,y,z directions
u^0, v^0, w^0 = midplane displacements in x,y,z directions
V_f, V_f^* = fiber volume fraction and effective fiber volume fraction
X, Y = bending-slope coefficients (amplitudes of ψ_x, ψ_y)
x, y, z = plate coordinates in longitudinal, transverse, and thickness (positive downward) directions
Z, Z_x, Z_y = z_n/h, z_{nx}/h, z_{ny}/h
z_n = neutral-surface position for transversely isotropic square plate
z_{nx}, z_{ny} = neutral-surface positions associated with $\epsilon_x = 0$ and $\epsilon_y = 0$, respectively
α, β = π/a, π/b
ϵ_j, ϵ_j^0 = strain component at arbitrary location and at midplane
κ_j = curvature component
ν_f, ν_m = fiber and matrix Poisson's ratios
ν_{12}, ν_{23} = major (longitudinal-transverse) and transverse-thickness Poisson's ratios
σ_i = stress component
ϕ_e, ϕ_e^i = typical dependent variable and its value at node i
ψ_x, ψ_y = bending slopes in xz and yz planes
$(\ )_{,x}$ = $\partial(\ )/\partial x$

Subscripts

i, j = 1,2,6 indices in contracted notation
k = 1 (t or tension), 2 (c or compression)
l = layer number

Received Jan. 10, 1980; presented as Paper 80-0685 at the AIAA/ASME/ASCE/AHS 21st Structures, Structural Dynamics, and Materials Conference, Seattle, Wash., May 12-14, 1980; revision received April 6, 1981.

*Benjamin H. Perkinson Professor of Engineering, School of Aerospace, Mechanical and Nuclear Engineering. Associate Fellow AIAA.

†Presently Professor, Dept. of Engineering Science and Mechanics, Virginia Polytechnic Institute and State University, Blacksburg, Va.

‡Graduate Research Assistant, Mechanical Engineering; presently, Engineer, Lear Fan Corp., Reno, Nev.

§Graduate Research Assistant, Mechanical Engineering; presently, Graduate Assistant, Engineering Science and Mechanics, Virginia Polytechnic Institute and State University, Blacksburg, Va.

Introduction

THE increasing use of composite materials in structures has led to the requirement of realistic mathematical modeling of the material behavior and incorporation of this more realistic model in structural analyses. Certain fiber-reinforced materials, especially those with very soft matrices (for example, cord-rubber composites and certain soft biological tissues), exhibit quite different elastic behavior depending upon whether the fiber-direction strain is tensile or compressive.[1-3] In such materials, the controlling phenomenon is fiber governed: tie-bar action for tension and column action for compression. As a first approximation, the stress-strain behavior of such materials is often represented as being bilinear, with different slopes (elastic properties) depending upon the sign of the fiber-direction strain. Such a

material is called a bimodulus composite material, and the fiber-governed symmetric-compliance model proposed in Ref. 4 has been shown to agree well with experimental data[3] for several materials with drastically different elastic properties in tension and compression.

To the best of the present investigators' knowledge, the only previous analyses of plates laminated of bimodulus composite materials are all limited to *thin* plates. Jones and Morgan[5] considered cylindrical bending of a finite-width cross-ply strip; Kincannon et al.[6] considered cross-ply elliptic plates. Rectangular plates were treated by Bert et al.[7] using a closed-form solution and by Reddy[8] using mixed finite elements.

Apparently the only previous analyses involving thick plates of bimodulus material are those of Shapiro[9] using a stress-function elasticity approach for isotropic circular plates and of Kamiya[10] using an energy approach for cylindrical bending of finite-width isotropic strips. Of course, for thick plates laminated of ordinary (not bimodulus) materials, there have been a number of analyses, such as those of Whitney,[11] Whitney and Pagano,[12] and Turvey,[13] for example. The analyses presented here are believed to be the first analyses of thick plates that are finite in two directions and laminated of bimodulus composite materials.

Formulation

The basic theory of laminated anisotropic thick plates used by Whitney and Pagano[12] is a modification of Yang, Norris, and Stavsky's theory,[14] which, in turn, is an extension of Mindlin's theory for isotropic plates.[15] All of these simple Timoshenko-type shear-deformation theories are based upon the following displacement field:

$$u(x,y,z) = u^0(x,y) + z\psi_x(x,y)$$
$$v(x,y,z) = v^0(x,y) + z\psi_y(x,y)$$
$$w(x,y,z) = w^0(x,y) \tag{1}$$

Here, x,y are rectangular coordinates in the plane of the plate, z is the thickness-direction coordinate measured downward from the midplane of the plate; u,v,w are the displacements in the respective x,y,z directions; u^0,v^0,w^0 are the corresponding midplane displacements; and ψ_x and ψ_y are the slopes in the xz and yz planes due to bending only.

Neglecting body forces, body moments, and surface shearing forces, one can write the equations of equilibrium as

$$N_{1,x}+N_{6,y}=0; \quad N_{6,x}+N_{2,y}=0; \quad Q_{x,x}+Q_{y,y}+q=0$$
$$M_{6,x}+M_{2,y}-Q_y=0; \quad M_{1,x}+M_{6,y}-Q_x=0 \tag{2}$$

Here q is the normal pressure, $(),_x$ denotes $\partial(\,)/\partial x$, and

$$(N_i,M_i) = \int_{-h/2}^{h/2} (1,z)\,\sigma_i\,\mathrm{d}z \qquad (i=1,2,6)$$
$$(Q_y,Q_x) = \int_{-h/2}^{h/2} (\sigma_4,\sigma_5)\,\mathrm{d}z \tag{3}$$

Here, h is the plate (laminate) thickness, and the so-called contracted subscript notation is employed to denote the stress components. Thus, σ_1 and σ_2 are in-plane normal stresses in the x and y directions, σ_6 is the in-plane shear stress associated with the x,y axes, and σ_4 and σ_5 are the thickness shear stresses in the yz and xz planes.

Each layer has monoclinic material symmetry, i.e., the only plane of symmetry existing is in the plane of the plate; thus, one can express the plate constitutive relations as

$$\begin{Bmatrix} N_i \\ M_i \end{Bmatrix} = \begin{bmatrix} A_{ij} & B_{ij} \\ B_{ij} & D_{ij} \end{bmatrix} \begin{Bmatrix} \epsilon_j \\ \kappa_j \end{Bmatrix} \qquad (i,j=1,2,6)$$
$$\begin{Bmatrix} Q_y \\ Q_x \end{Bmatrix} = \begin{bmatrix} K_4^2S_{44} & K_4K_5S_{45} \\ K_4K_5S_{45} & K_5^2S_{55} \end{bmatrix} \begin{Bmatrix} \epsilon_4 \\ \epsilon_5 \end{Bmatrix} \tag{4}$$

The $A_{ij},B_{ij},D_{ij},S_{ij}$ are the respective in-plane, bending-stretching coupling, bending or twisting, and thickness-shear stiffnesses defined as follows:

$$(A_{ij},B_{ij},D_{ij}) = \int_{-h/2}^{h/2} (1,z,z^2)\,Q_{ijkl}\,\mathrm{d}z \qquad (i,j=1,2,6)$$
$$S_{ij} = \int_{-h/2}^{h/2} Q_{ijkl}\,\mathrm{d}z \qquad (i,j=4,5) \tag{5}$$

Here, Q_{ijkl} denotes the plane-stress reduced stiffness, where ij refers to the position in the stress-strain-relation array [analogous to Eqs. (4)], k refers to the sign of the fiber-direction strain ($1\sim+$, $2\sim-$), and l is the layer number. (The theories of Refs. 12 and 14 differ in the kind of stiffnesses used; Wang and Chou[16] showed that the plane-stress reduced stiffnesses used here and in Ref. 12 are most appropriate.)

The linear equations for the kinematics of deformation are

$$\epsilon_1^0 = u^0,_x; \quad \epsilon_2^0 = v^0,_y; \quad \epsilon_6^0 = u^0,_y + v^0,_x$$
$$\kappa_1 = \psi_{x,x}; \quad \kappa_2 = \psi_{y,y}; \quad \kappa_6 = \psi_{x,y} + \psi_{y,x}$$
$$\epsilon_4 = w^0,_y + \psi_y; \quad \epsilon_5 = w^0,_x + \psi_x \tag{6}$$

Equations (1-6) plus those of Appendix A constitute the appropriate theory, in differential-equation form, for the class of plates considered here (linear, thick, laminated, anisotropic, bimodulus).

Closed-Form Solution for Cross-Ply Laminate

Here, we consider the particular case of a cross-ply laminate, i.e., one in which some of the fibers are oriented along the x axis and the remainder along the y axis. Then, the terms with subscripts 16, 26, and 45 vanish from the symmetric arrays in Eqs. (4). For bimodulus-material cross-ply laminates, Eqs. (5) are integrated as in Appendix A and depend upon the neutral-surface locations, Z_x and Z_y, as well as the Q_{ijkl}.

Tentatively assuming that the neutral-surface locations are independent of x and y, one can combine Eqs. (2), (4), and (6) to yield the following governing equations in terms of the midplane displacements (u^0,v^0,w^0) and bending slopes (ψ_y and ψ_x):

$$[L_{rs}]\{u^0,v^0,w^0,\psi_y,\psi_x\}^T = \{0,0,q,0,0\}^T \tag{7}$$

where $[L_{rs}]$ is a symmetric differential operator matrix with the following elements:

$$L_{11}=A_{11}\mathrm{d}_x^2+A_{66}\mathrm{d}_y^2; \quad L_{12}=(A_{12}+A_{66})\mathrm{d}_x\mathrm{d}_y; \quad L_{13}=0$$
$$L_{14}=(B_{12}+B_{66})\mathrm{d}_x\mathrm{d}_y; \quad L_{15}=B_{11}\mathrm{d}_x^2+B_{66}\mathrm{d}_y^2$$
$$L_{22}=A_{66}\mathrm{d}_x^2+A_{22}\mathrm{d}_y^2; \quad L_{23}=0 \quad L_{24}=B_{66}\mathrm{d}_x^2+B_{22}\mathrm{d}_y^2$$
$$L_{25}=L_{14}; \quad L_{33}=-K_5^2S_{55}\mathrm{d}_x^2-K_4^2S_{44}\mathrm{d}_y^2$$
$$L_{34}=-K_4^2S_{44}\mathrm{d}_y; \quad L_{35}=-K_5^2S_{55}\mathrm{d}_x$$
$$L_{44}=D_{66}\mathrm{d}_x^2+D_{22}\mathrm{d}_y^2-K_4^2S_{44}; \quad L_{45}=(D_{12}+D_{66})\mathrm{d}_x\mathrm{d}_y$$
$$L_{55}=D_{11}\mathrm{d}_x^2+D_{66}\mathrm{d}_y^2-K_5^2S_{55}; \quad \mathrm{d}_x=\partial(\,)/\partial x; \quad \mathrm{d}_y=\partial(\,)/\partial y \tag{8}$$

For a plate hinged flexurally, but free to move in a direction normal to each edge (SS3 in Hoff's notation[17]), the boundary conditions are

$$N_1(0,y)=N_1(a,y)=0; \quad u^0(x,0)=u^0(x,b)=0$$
$$v^0(0,y)=v^0(a,y)=0; \quad N_2(x,0)=N_2(x,b)=0$$
$$w^0(0,y)=w^0(a,y)=0; \quad w^0(x,0)=w^0(x,b)=0$$
$$\psi_y(0,y)=\psi_y(a,y)=0; \quad M_2(x,0)=M_2(x,b)=0$$
$$M_1(0,y)=M_1(a,y)=0; \quad \psi_x(x,0)=\psi_x(x,b)=0 \tag{9}$$

In deriving Eq. (7), we implied that the A_{ij}, B_{ij}, and D_{ij} were all independent of x and y and thus that the neutral-surface locations associated with the x and y directions remain constant. The criteria for this condition to exist are obtained from the following definitions of the respective neutral-surface locations for $\epsilon_x=0$ and for $\epsilon_y=0$:

$$\epsilon_1^0+z_{nx}\kappa_1=0; \quad \epsilon_2^0+z_{ny}\kappa_2=0 \tag{10}$$

Thus, the following criteria result:

$$z_{nx}=-\epsilon_1^0/\kappa_1=-u^0{}_{,x}/\psi_{x,x}=\text{const}$$
$$z_{ny}=-\epsilon_2^0/\kappa_2=-v^0{}_{,y}/\psi_{y,y}=\text{const} \tag{11}$$

(In *general*, z_{nx} and z_{ny} are not independent of x and y; then the finite-element analysis presented in the next section may be used.)

The normal-pressure loading is sinusoidally distributed as

$$q=q_0 \sin \alpha x \sin \beta y \tag{12}$$

where $\alpha \equiv \pi/a$, $\beta \equiv \pi/b$. The governing equations, Eq. (7), with pressure distribution given by Eq. (12), boundary conditions as Eqs. (9), and neutral-surface location criteria as Eqs. (11) are all satisfied exactly in closed form by the following set of functions.

$$u^0=U \cos \alpha x \sin \beta y \qquad \psi_y=Y \sin \alpha x \cos \beta y$$
$$v^0=V \sin \alpha x \cos \beta y \qquad \psi_x=X \cos \alpha x \sin \beta y$$
$$w^0=W \sin \alpha x \sin \beta y \tag{13}$$

Then, the differential equation set, Eq. (7), reduces to the following algebraic form:

$$[C_{rs}]\{U,V,W,Y,X\}^T=\{0,0,q_0,0,0\}^T \tag{14}$$

Here, $[C_{rs}]$ is a symmetric matrix with coefficients

$$C_{11}=A_{11}\alpha^2+A_{66}\beta^2; \; C_{12}=(A_{12}+A_{66})\alpha\beta; \; C_{13}=0;$$
$$C_{14}=(B_{12}+B_{66})\alpha\beta; \; C_{15}=B_{11}\alpha^2+B_{66}\beta^2;$$
$$C_{22}=A_{66}\alpha^2+A_{22}\beta^2; \; C_{23}=0; \; C_{24}=B_{66}\alpha^2+B_{22}\beta^2;$$
$$C_{25}=C_{14}; \; C_{33}=K_5^2S_{55}\alpha^2+K_4^2S_{44}\beta^2; \; C_{34}=K_4^2S_{44}\beta;$$
$$C_{35}=K_5^2S_{55}\alpha; \; C_{44}=D_{66}\alpha^2+D_{22}\beta^2+K_4^2S_{44};$$
$$C_{45}=(D_{12}+D_{66})\alpha\beta; \; C_{55}=D_{11}\alpha^2+D_{66}\beta^2+K_5^2S_{55} \tag{15}$$

Finite-Element Analysis

Here, we present a mixed finite-element model associated with Eqs. (1-4) governing the bending of laminated, thick composite plates. The word "mixed" implies that independent approximations are used for all of the variables, u,v,w,ψ_x, and ψ_y. Using the thin-plate equations of layered composite plates, and treating

$$w_{,x}+\psi_x=0, \quad w_{,y}+\psi_y=0 \tag{16}$$

as constraints, Reddy[18] presented a variational formulation of Eqs. (1-4). That is, the thick-plate theory can be interpreted as one resulting from the thin-plate theory by treating the slope-displacement relations as constraints. The Lagrange multipliers associated with these constraints are found to be the thickness-shear stress resultants Q_x and Q_y. The model described here is essentially the same as in Ref. 18 (ordinary-material, thick plate) and Ref. 19 (preliminary results for bimodulus-material, thin plates).

Suppose that the region occupied by the plate is given by $\Omega X(-h/2, h/2)$, where Ω denotes the middle plane ($z=0$). As noted earlier, the coefficients A_{ij}, B_{ij}, and D_{ij} are integrated through the entire thickness. Hence, we divide the plate into a finite number of elements, denoted by Ω_e. Over each element Ω_e, we assume that the variables u,v,w,ψ_x, and ψ_y are interpolated by expressions of the form

$$\phi^e=\sum_i^n \mathfrak{N}_i \phi_e^i \tag{17}$$

where ϕ^e denotes the restriction of a typical variable to Ω_e, ϕ_e^i its value at node i (of element Ω_e), and $\mathfrak{N}_i$ are the linearly independent interpolation functions associated with the typical element. Because we are concerned here with rectangular plates, the typical element is chosen to be the four-node ($n=4$) quadrilateral element.

Substituting expressions of the form in Eq. (17) for u,v,w,ψ_x, and ψ_y into the total potential energy associated with the case of a thick, cross-ply laminate

$$\frac{1}{2}\int_\Omega \left\{A_{11}\left(\frac{\partial u}{\partial x}\right)^2+A_{66}\left(\frac{\partial u}{\partial y}\right)^2+2A_{12}\frac{\partial u}{\partial x}\frac{\partial v}{\partial y}+2A_{66}\frac{\partial u}{\partial y}\frac{\partial v}{\partial x}\right.$$
$$+A_{22}\left(\frac{\partial v}{\partial y}\right)^2+A_{66}\left(\frac{\partial v}{\partial x}\right)^2+\frac{\partial u}{\partial x}\left(B_{11}\frac{\partial \psi_x}{\partial x}+B_{12}\frac{\partial \psi_y}{\partial y}\right)$$
$$+B_{66}\left(\frac{\partial u}{\partial y}+\frac{\partial v}{\partial x}\right)\left(\frac{\partial \psi_x}{\partial y}+\frac{\partial \psi_y}{\partial x}\right)+\frac{\partial v}{\partial y}\left(B_{12}\frac{\partial \psi_x}{\partial x}+B_{22}\frac{\partial \psi_y}{\partial y}\right)$$
$$+\frac{\partial \psi_x}{\partial x}\left(B_{11}\frac{\partial u}{\partial x}+B_{12}\frac{\partial v}{\partial y}\right)+B_{66}\left(\frac{\partial \psi_x}{\partial y}+\frac{\partial \psi_y}{\partial x}\right)\left(\frac{\partial u}{\partial y}+\frac{\partial v}{\partial x}\right)$$
$$+\frac{\partial \psi_y}{\partial y}\left(B_{12}\frac{\partial u}{\partial x}+B_{22}\frac{\partial v}{\partial y}\right)+D_{11}\left(\frac{\partial \psi_x}{\partial x}\right)^2+D_{66}\left(\frac{\partial \psi_x}{\partial y}\right)^2$$
$$+2D_{12}\frac{\partial \psi_x}{\partial x}\frac{\partial \psi_y}{\partial y}+2D_{66}\frac{\partial \psi_x}{\partial y}\frac{\partial \psi_y}{\partial x}+D_{22}\left(\frac{\partial \psi_y}{\partial y}\right)^2+D_{66}\left(\frac{\partial \psi_y}{\partial x}\right)$$
$$\left.+A_{55}\left(\frac{\partial w}{\partial x}+\psi_x\right)^2+A_{44}\left(\frac{\partial w}{\partial y}+\psi_y\right)^2\right\}dx\,dy+\int_\Omega qw\,dx\,dy \tag{18}$$

we obtain, for each element,

$$[K^e]\{\Delta^e\}=\{F^e\} \tag{19}$$

where $\{\Delta^e\}=\{u_i^e,v_i^e,w_i^e,\psi_{xi}^e,\psi_{yi}^e\}^T$, and

$$K_{ij}^{11}=A_{11}\mathcal{S}_{ij}^x+A_{66}\mathcal{S}_{ij}^y, \quad K_{ij}^{12}=A_{12}\mathcal{S}_{ij}^{xy}+A_{66}\mathcal{S}_{ji}^{xy}$$
$$K_{ij}^{13}=0, \; K_{ij}^{14}=B_{11}\mathcal{S}_{ij}^x+B_{66}\mathcal{S}_{ij}^y, \; K_{ij}^{15}=B_{12}\mathcal{S}_{ij}^{xy}+B_{66}\mathcal{S}_{ji}^{xy}$$
$$K_{ij}^{22}=A_{22}\mathcal{S}_{ij}^y+A_{66}\mathcal{S}_{ij}^x, \; K_{ij}^{23}=0, \; K_{ij}^{24}=B_{66}\mathcal{S}_{ij}^{xy}+B_{12}\mathcal{S}_{ji}^{xy}$$
$$K_{ij}^{25}=B_{66}\mathcal{S}_{ij}^x+B_{22}\mathcal{S}_{ij}^y, \; K_{ij}^{33}=A_{55}\mathcal{S}_{ij}^x+A_{44}\mathcal{S}_{ij}^y, \; K_{ij}^{34}=A_{55}\mathcal{S}_{ij}^{x0}$$
$$K_{ij}^{35}=A_{44}\mathcal{S}_{ij}^{y0}, \; K_{ij}^{44}=D_{11}\mathcal{S}_{ij}^x+D_{66}\mathcal{S}_{ij}^y+A_{55}\mathcal{S}_{ij}^0$$

$$K_{ij}^{45}=D_{12}\mathcal{S}_{ij}^{xy}+D_{66}\mathcal{S}_{ji}^{xy},\quad K_{ij}^{55}=D_{66}\mathcal{S}_{ij}^{x}+D_{22}\mathcal{S}_{ij}^{y}+A_{44}\mathcal{S}_{ij}^{0}$$

$$F_i^3=\int_{\Omega_e} q\mathfrak{N}_i\,dx,dy,\quad F_i^\alpha=0,\quad \alpha=1,2,3,4,5,$$

$$A_{\alpha\beta}=K_\alpha K_\beta \mathcal{S}_{\alpha\beta},\ (\alpha,\beta=4,5)$$

$$\mathcal{S}_{ij}^{\xi\eta}=\int_{\Omega_e}\mathfrak{N}_{i,\xi}\mathfrak{N}_{j,m\eta}\,dxdy\ (\xi,\eta=0,x,y),\quad \mathcal{S}_{ij}^{0}=\mathcal{S}_{ij}^{00} \tag{20}$$

The element equations, Eqs. (19), are assembled in the usual manner, and boundary conditions are applied before solution of the equations.

Numerical Results

As the first example, we take the case of a homogeneous (single-layer), square plate of transversely isotropic bimodulus material. The plane of isotropy is parallel to the midplane of the plate, and the in-plane Poisson's ratio is zero. Then, the closed-form solution reduces to the simplified form of the single equation, Eq. (B6), presented in Appendix B. The neutral-surface location is independent of the plate thickness and of the moduli ratios (E_t/E_c and G_{zc}/E_c) (see Table 1). Also, there is good agreement among the results obtained with all three approaches in Table 1. The dimensionless deflection (defined to be normalized by E_c) decreases as E_t/E_c and G_{zc}/E_c are increased (see Table 2). Again, the agreement between the finite-element and closed-form solutions is excellent, whereas the simplified solution has slightly lower deflection values.

Examples of some actual bimodulus materials are aramid cord-rubber and polyester cord-rubber with material properties listed in Table 3. The data are based on test results of Patel et al.[3] and were obtained by the data-reduction procedure of Model 2 in Ref. 4, except for the thickness-shear moduli, which were estimated as explained in Appendix C.

For single-layer plates with the fibers oriented parallel to the x axis (Table 4) and cross-ply plates with stacking sequence as described in Appendix A (Table 5), Z_x, the dimensionless neutral-surface location for $\epsilon_x=0$, decreases slightly with increasing aspect ratio (a/b). In contrast Z_y, the dimensionless neutral-surface location for $\epsilon_y=0$, decreases considerably in magnitude and dimensionless deflection increases with increasing a/b. The agreement between the closed-form and finite-element results for both neutral-surface position and deflection is extremely good, as can be seen in Tables 4 and 5. Thus, the finite-element analysis has been soundly validated, and can now be used for more complicated combinations of loading, geometry, and boundary conditions not amenable to closed-form solutions.

The aramid-rubber plates, in both the single-ply and cross-ply cases, are seen to have noticeably larger values of Z_x than the polyester-rubber plates. This result is undoubtedly due to the more pronounced bimodulus effect in the fiber-direction Young's modulus of the aramid-rubber. Also, it is interesting to observe that there are only very slight differences in Z_x and deflection in going from a single layer to a cross-ply laminate. This result is in contrast to the behavior of the polyester-rubber results and in considerable contrast to ordinary materials (which, of course, have $Z_x=0$ for the single-layer case). The most pronounced change in going from the single-layer to the two-layer case is the drastic decrease in Z_y for the aramid-rubber.

The reader is cautioned that in the case of the closed-form solution, deflections due to various sinusoidally distributed loadings *cannot* be superimposed for bimodulus-material plates. The reason superposition is not valid here is that the necessary conditions, Eqs. (11), for homogeneity of neutral-surface locations are not valid under superposition conditions, since, in general

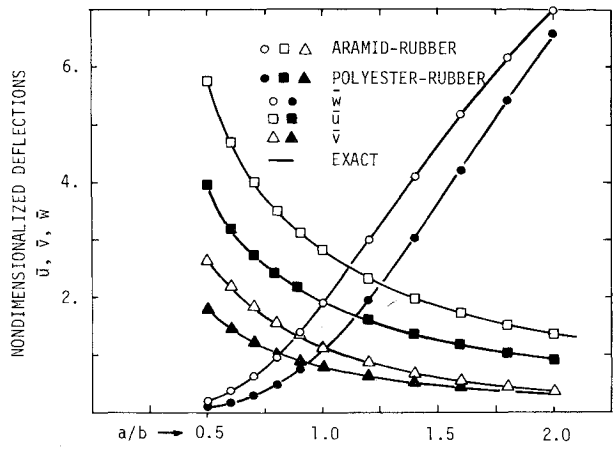

Fig. 1 Effect of plate aspect ratio a/b on dimensionless displacements ($\bar{w}=10^2\,w_{max}E_{22c}h^3/q_0b^4$, $\bar{u}=2\times10^4\,u_{max}/w_{max}$, $\bar{v}=2\times10^4\,v_{max}/w_{max}$) of aramid-rubber and polyester-rubber rectangular plates under sinusoidally distributed loading ($b/h=100$, single-layer).

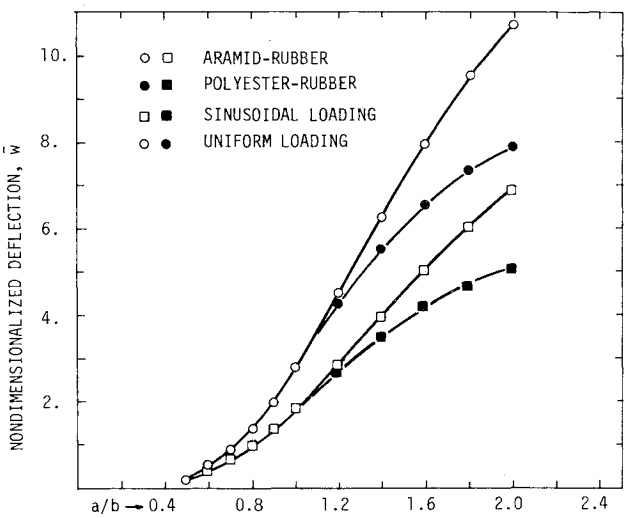

Fig. 2 Effect of plate aspect ratio a/b on dimensionless displacement $\bar{w}$ of aramid-rubber and polyester-rubber two-layer, cross-ply rectangular plates under uniform and sinusoidally distributed loadings ($b/h=100$).

$$Z_x=\frac{Z_x^{(1)}\psi_{x,x}^{(1)}(x,y)+Z_x^{(2)}\psi_{x,x}^{(2)}(x,y)}{\psi_{x,x}^{(1)}(x,y)+\psi_{x,x}^{(2)}(x,y)}\neq\text{const} \tag{21}$$

even though $Z_x^{(1)}$, $Z_x^{(2)}$,... for the various individual Fourier components are constants. However, the finite-element solution is not subject to these limitations, since it provides for stepwise variation in neutral-surface location.

In every case investigated, all three of the displacements for plates of aramid-rubber are greater than the corresponding ones for polyester-rubber as shown in Figs. 1 and 2. For the nondimensionalizations used for the displacements, the in-plane displacements ($\bar{u}$ and $\bar{v}$) decreases as the aspect ratio is increased, while the normal deflection ($\bar{w}$) increases. The excellent agreement between the exact and finite-element results is also demonstrated in Fig. 1.

For small aspect ratios, the normal deflection for sinusoidally distributed loading is nearly the same as that for uniformly distributed loading, as may be seen in Fig. 2. Of course, the uniform-distribution results displayed in this figure were necessarily obtained by finite-element analysis only, as explained heretofore in this section.

Table 1 Comparison of neutral-surface locations for transversely isotropic square plates

$\frac{E_t}{E_c}=\frac{G_{zt}}{G_{zc}}$	Neutral-surface location Z		
	$G_{zc}/E_c=0.1$	0.3	0.5
	Exact closed-form solution:		
0.5	−0.08578	−0.08578	−0.08578
1.0	0	0	0
2.0	+0.08578	+0.08578	+0.08578
	Simplified approximate solution:		
0.5	−0.08579	−0.08579	−0.08579
1.0	0	0	0
2.0	+0.08579	+0.08579	+0.08579
	Mixed finite-element solution:		
0.5	−0.08578	−0.08578	−0.08578
1.0	0	0	0
2.0	+0.08578	+0.08578	+0.08578

Table 2 Comparison of maximum deflections for transversely isotropic square plates ($h/b=0.1$, $K^2=5/6$)

$\frac{E_t}{E_c}=\frac{G_{zt}}{G_{zc}}$	Dimensionless deflection WE_ch^3/q_0b^4		
	$G_{zc}/E_c=0.1$	0.3	0.5
	Exact closed-form solution:		
0.5	0.05348	0.04774	0.04660
1.0	0.03688	0.03283	0.03201
2.0	0.02674	0.02387	0.02330
	Simplified approximate solution:		
0.5	0.05004	0.04660	0.04591
1.0	0.03445	0.03202	0.03153
2.0	0.02530	0.02342	0.02296
	Mixed finite-element solution:		
0.5	0.05329	0.04743	0.04626
1.0	0.03675	0.03261	0.03178
2.0	0.02664	0.02371	0.02313

Table 3 Elastic properties for two tire cord-rubber, unidirectional, bimodulus composite materials[a]

Property and units	Aramid-rubber		Polyester-rubber	
	Tens.	Compr.	Tens.	Compr.
Longitudinal Young's modulus, GPa	3.58	0.0120	0.617	0.0369
Transverse Young's modulus, GPa	0.00909	0.0120	0.00800	0.0106
Major Poisson's ratio, dimensionless[b]	0.416	0.205	0.475	0.185
Longitudinal-transverse shear modulus, GPa[c]	0.00370	0.00370	0.00262	0.00267
Transverse-thickness shear modulus, GPa	0.00290	0.00499	0.00233	0.00475

[a]Fiber-direction tension is denoted by Tens., and fiber-direction compression by Compr. [b]The minor Poisson's ratio is assumed to be given by the reciprocal relation. [c]The longitudinal-thickness shear modulus is taken to be equal to the longitudinal-transverse shear modulus.

Table 4 Neutral-surface positions and dimensionless deflections for rectangular plates of single-layer 0° aramid-rubber and polyester-rubber, as determined by two different methods (thickness/width, $h/b=0.1$; $K^2=5/6$)

Aspect ratio	Z_x		Z_y		$WE_{22c}h^3/q_0b^4$	
	C.F.[a]	F.E.[b]	C.F.	F.E.	C.F.	F.E.
			Aramid-rubber:			
0.5	0.4453	0.4454	−0.3304	−0.3007	0.002544	0.002750
0.7	0.4447	0.4447	−0.2564	−0.2419	0.007393	0.007712
1.0	0.4420	0.4420	−0.1671	−0.1614	0.02046	0.02083
1.4	0.4363	0.4363	−0.1015	−0.09919	0.04313	0.04335
2.0	0.4253	0.4254	−0.05813	−0.05727	0.07250	0.07236
			Polyester-rubber:			
0.5	0.3044	0.3045	−0.1597	−0.1234	0.001529	0.001971
0.7	0.3042	0.3044	−0.1426	−0.1198	0.004283	0.005075
1.0	0.3029	0.3031	−0.1061	−0.09586	0.01303	0.01430
1.4	0.2999	0.3001	−0.07329	−0.06941	0.03348	0.03492
2.0	0.2934	0.2936	−0.04959	−0.04828	0.06925	0.07003

[a]C.F. denotes closed-form solution. [b]F.E. signifies finite-element solution.

Table 5 Neutral-surface positions and dimensionless deflections for rectangular plates of two-layer cross-ply aramid-rubber and polyester-rubber, as determined by two different methods (thickness/width, $h/b=0.1$; $K^2=5/6$)

Aspect ratio	Z_x		Z_y		$WE_{22c}h^3/q_0b^4$	
	C.F.[a]	F.E.[b]	C.F.	F.E.	C.F.	F.E.
			Aramid-rubber:			
0.5	0.4433	0.4431	−0.06343	−0.06223	0.002472	0.002576
0.7	0.4418	0.4418	−0.04794	−0.04778	0.007072	0.007220
1.0	0.4384	0.4384	−0.03437	−0.03430	0.01957	0.01972
1.4	0.4326	0.4325	−0.02470	−0.02477	0.04185	0.04190
2.0	0.4219	0.4219	−0.01735	−0.01734	0.07151	0.07137
			Polyester-rubber:			
0.5	0.3650	0.3652	−0.1285	−0.1256	0.002539	0.002732
0.7	0.3638	0.3639	−0.1097	−0.1089	0.007288	0.007575
1.0	0.3613	0.3613	−0.09526	−0.09502	0.01933	0.01966
1.4	0.3571	0.3570	−0.08660	−0.08660	0.03674	0.03707
2.0	0.3491	0.3490	−0.08150	−0.08150	0.05301	0.05337

[a]C.F. denotes closed-form solution. [b]F.E. signifies finite-element solution.

Concluding Remarks

Both finite-element and closed-form solutions are found for thick, rectangular plates of single layer and cross-ply laminated of bimodulus materials. Excellent agreement is obtained, and thus the finite-element formulation of this problem is considered to be validated against an accurate benchmark.

The research reported here has recently been extended to 1) free vibration[20] and 2) thermal bending due to changes in midplane temperature and in gradient through the thickness.[21]

Appendix A: Derivation of the Plate Stiffnesses for a Two-Layer Cross-Ply Laminate of Bimodulus Material

In laminates containing bimodulus materials, the results of evaluating the integrals for the plate stiffnesses, Eqs. (5), are more complicated than those for ordinary-material laminates, because the individual-layer, plane-stress-reduced stiffnesses can take on either one of two different values depending upon the appropriate neutral-surface locations. Here, we derive the expressions for a two-layer, cross-ply laminate (see Fig. A1). Each layer has the same thickness and the same bimodulus orthotropic elastic properties with respect to the fiber direction. The bottom layer is denoted as layer 1, i.e., $l=1$ in Q_{ijkl}, is oriented in the x direction, and occupies the thickness-direction interval from $z=0$ to $z=h/2$, where z is measured positively downward from the midplane. The top layer ($l=2$) is oriented in the y direction and is located from $z=-h/2$ to $z=0$. In the case considered, it is assumed that the upper portion of the top layer ($l=2$) is in compression ($k=2$ in Q_{ijkl}) in the fiber direction and that the lower portion of the top layer is in tension ($k=1$), whereas the inner portion of the bottom layer ($l=1$) is in compression ($k=2$) and the outer portion of this layer in tension ($k=1$). The four regions are summarized in Table A1.

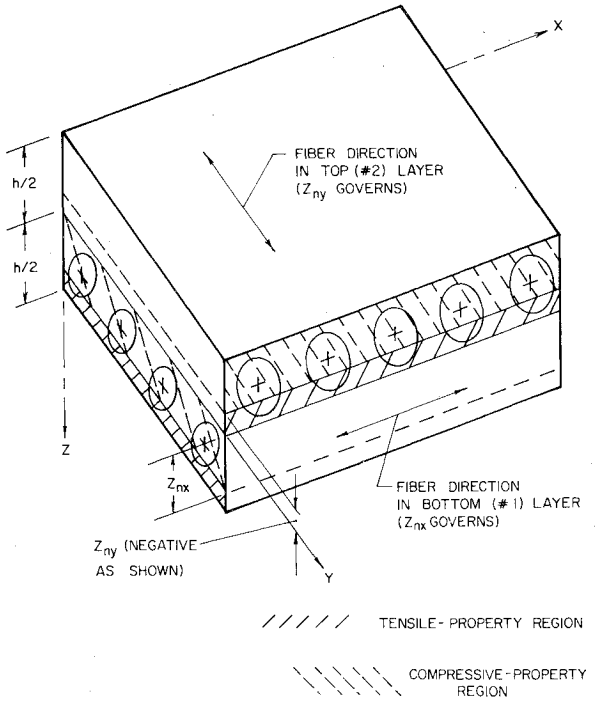

Fig. A1 Schematic of an element of a two-layer, cross-ply plate showing the tensile-property and compressive-property regions and z_{nx} and z_{ny}, the neutral-surface positions for $\epsilon_x=0$ and $\epsilon_y=0$, respectively.

Table A1 Summary of regions and their corresponding fiber-direction strain states

Layer	Region	Fiber-direction tension or compression
$l=2$	$-h/2$ to z_{ny}	Compression ($k=2$)
$l=2$	z_{ny} to 0	Tension ($k=1$)
$l=1$	0 to z_{nx}	Compression ($k=2$)
$l=1$	z_{nx} to $h/2$	Tension ($k=1$)

The quantity z_{nx}, the location of the neutral surface for $\epsilon_x=0$, is positive; z_{ny}, the location of the neutral surface for $\epsilon_y=0$, is negative.

Thus, the integral for A_{ij} in Eqs. (5) is subdivided into four regions, in each of which the plane-stress reduced stiffnesses Q_{ijkl} are constant.

$$A_{ij}=\int_{-h/2}^{z_{ny}} Q_{ij22}\,dz+\int_{z_{ny}}^{0} Q_{ij12}\,dz+\int_{0}^{z_{nx}} Q_{ij21}\,dz+\int_{z_{nx}}^{h/2} Q_{ij11}\,dz=(Q_{ij11}+Q_{ij22})(h/2)+(Q_{ij21}-Q_{ij11})z_{nx}+(Q_{ij22}-Q_{ij12})z_{ny} \tag{A1}$$

Introducing $Z_x=z_{nx}/h$ and $Z_y=z_{ny}/h$, one obtains

$$A_{ij}/h=\tfrac{1}{2}(Q_{ij22}+Q_{ij11})+(Q_{ij21}-Q_{ij11})Z_x+(Q_{ij22}-Q_{ij12})Z_y \tag{A2}$$

In similar fashion, the next two integrals in Eqs. (5) become

$$4B_{ij}/h^2=\tfrac{1}{2}(Q_{ij11}-Q_{ij22})+2(Q_{ij21}-Q_{ij11})Z_x^2+2(Q_{ij22}-Q_{ij12})Z_y^2 \tag{A3}$$

$$12D_{ij}/h^3=\tfrac{1}{2}(Q_{ij11}+Q_{ij22})+4(Q_{ij21}-Q_{ij11})Z_x^3+4(Q_{ij21}-Q_{ij12})Z_y^3 \tag{A4}$$

The expression for S_{ij}/h is the same as for A_{ij}/h, Eq. (A2).

To apply Eqs. (A2-A4) to a single-layer plate with the fibers oriented in the x direction, it is merely necessary to set $Z_y=0$. In deriving these equations, we assumed that $Z_x\geq 0$ and $Z_y\leq 0$. In the event that the final results obtained for Z_x and Z_y did not meet these conditions, obviously Eqs. (A2-A4) would not be valid, and it would become necessary to investigate another of the other three possible cases:

$$Z_x\geq 0 \text{ and } Z_y\geq 0$$

$$Z_x\leq 0 \text{ and } Z_y\leq 0$$

$$Z_x\leq 0 \text{ and } Z_y\geq 0$$

Fortunately, however, in all of the problems treated here, the conditions for the case derived in this appendix are satisfied.

Appendix B: Reduction of Closed-Form Solution for Single-Layer Transversely Isotropic Material

In order to obtain simple, concise expressions for the neutral-surface location and the deflection, the closed-form equations given in the body of the paper are reduced to the special case of a square plate made of a transversely isotropic bimodulus material with an in-plane Poisson's ratio of zero.

Then

$$A_{11}=A_{22}=A, \quad A_{12}=0, \quad A_{66}=A/2$$
$$B_{11}=B_{22}=B, \quad B_{12}=0, \quad B_{66}=B/2$$
$$D_{11}=D_{22}=D, \quad D_{12}=0, \quad D_{66}=D/2$$
$$S_{44}=S_{55}=S, \quad S_{45}=0 \tag{B1}$$

Now, Eqs. (15) reduce to the following, because $\beta=\alpha$:

$$C_{11}=(3/2)A\alpha^2, \quad C_{12}=(1/2)A\alpha^2, \quad C_{13}=0,$$
$$C_{14}=(1/2)B\alpha^2, \quad C_{15}=(3/2)B\alpha^2, \quad C_{ji}=C_{ij}, \quad C_{22}=C_{11}$$
$$C_{23}=0, \quad C_{24}=C_{15}, \quad C_{25}=C_{14}, \quad C_{33}=2K^2S\alpha^2$$
$$C_{34}=K^2S\alpha, \quad C_{35}=C_{34}, \quad C_{44}=(3/2)D\alpha^2+K^2S$$
$$C_{45}=(1/2)D\alpha^2, \quad C_{55}=C_{44} \tag{B2}$$

The biaxial symmetry of this special case requires

$$b=a, \quad \beta=\alpha, \quad V=U, \quad Y=X, \quad z_{nx}=z_{ny}=z_n \tag{B3}$$

Using Eqs. (B2) and (B3) in the first two of Eqs. (14), one finds that for this special case

$$z_{nx}=z_{ny}=B/A=z_n \tag{B4}$$

Using the fourth equation of Eqs. (14), one obtains

$$X/W=\frac{-K^2S\alpha}{2(D-Bz_n)\alpha^2+K^2S} \tag{B5}$$

It is noted that the bending slope vanishes for both $S=0$ and $1/S=0$.

Finally, the third of Eqs. (14) yields

$$W=\frac{q_0}{4(D-Bz_n)\alpha^4}\left[1+2(D-Bz_n)(\alpha^2/K^2S)\right] \tag{B6}$$

It is seen that the quantity in front of the first bracket on the right side of Eq. (B6) is equal to the deflection of a thin isotropic plate. The second term inside the brackets is the fractional increase in deflection due to thickness-shear deformation, which obviously increases as G_z is decreased. The quantity $D-Bz_n$ is the so-called reduced bending stiffness, first obtained for laminated isotropic thin plates by Pister.[22]

For the present case, Eqs. (A2-A4) become

$$A/h=\bar{Q}+Z\Delta Q, \quad 4B/h^2=-(1/2)(1-4Z^2)\Delta Q \tag{B7}$$
$$12D/h^3=\bar{Q}+4Z^3\Delta Q$$

Here

$$\bar{Q}=(1/2)(Q_c+Q_t), \quad \Delta Q\equiv Q_c-Q_t \tag{B8}$$

Combining Eqs. (B4) and (B7), one obtains the following quadratic expression for Z:

$$Z=-(\bar{Q}/Q)\pm[(\bar{Q}/\Delta Q)^2-(1/4)]^{1/2} \tag{B9}$$

Also

$$S/h=(1/2)(G_{zc}+G_{zt})+Z(G_{zc}-G_{zt}) \tag{B10}$$

Appendix C: Method of Estimating Transverse-Thickness Shear Moduli

In the tests reported by Patel et al.[3] only in-plane compliances were measured. Thus, one must estimate the values for the thickness-shear moduli that are needed for the thick-plate analysis.

A reasonable engineering assumption is to assume that an individual composite-material layer is transversely isotropic with the plane of isotropy being the cross-sectional plane, i.e., the plane normal to the fibers. Therefore, the longitudinal-thickness shear modulus (G_{13}) is equal to the in-plane (longitudinal-transverse) shear modulus (G_{12}).

Estimation of the other thickness-shear modulus is more complicated. One can use the well-known isotropic relation for the transverse-thickness shear modulus G_{23k} in terms of the thickness-direction Young's modulus E_{3k} and transverse-thickness Poisson's ratio ν_{23k} provided the latter two quantities are known:

$$G_{23k}=E_{3k}/[2(1+\nu_{23k})] \tag{C1}$$

In view of the transverse-isotropy assumption mentioned above, it can be assumed that $E_{3k}=E_{2k}$, which was obtained from the in-plane tests.

Foye[23] presented a relation for ν_{23} which can be rewritten in the following form, which is more convenient for the present purpose:

$$\nu_{23k}=\nu_{12k}+\frac{[(\nu_m/E_m)-(\nu_f/E_f)]\nu_m(1-\nu_m)}{\dfrac{1-\nu_m^2}{E_m(1-V_f)}+\dfrac{1}{E_fV_f}-\dfrac{\nu_m}{E_m}\dfrac{\nu_f}{E_f}} \tag{C2}$$

Data for only E_f, E_m, and V_f can be found in Ref. 3. However, it is reasonable to use a value of 0.499 for ν_m of rubber. Thus, the only unknown quantity on the right side of Eq. (C2) is ν_f, which could be computed from the following rule-of-mixtures expression for ν_{12k} known to be very accurate for polymer-matrix composites:

$$\nu_{12k}=\nu_{fk}V_f+\nu_m(1-V_f) \tag{C3}$$

The rule-of-mixtures expression for the longitudinal Young's modulus is also known to be accurate for polymer-matrix composites:

$$E_{1k}=E_{fk}V_f+E_m(1-V_f) \tag{C4}$$

Unfortunately, however, for the data of Ref. 3, the measured values of E_{1t} (tension) were *higher* than predicted with Eq. (C4). Thus, we used Eq. (C4) to obtain an effective fiber volume fraction V_f^*, and then used this effective value to predict E_{fc} (compression) and ν_{ft} and ν_{fc}. However, using either V_f or V_f^* in Eq. (C3), one obtains negative ν_{ft} and ν_{fc} values which, although admissible thermodynamically, do not seem likely or plausible to the authors. Thus, due to the loose nature of the cord, we assumed that the cord was not restrained by the matrix. Therefore, instead of obtaining ν_{fk} from Eq. (C3), we obtained it from

$$\nu_{fk}=\nu_{12k}/V_f^* \tag{C5}$$

Sample calculations for aramid-rubber in compression are as follows. From Eq. (C4) for $k=t$:

$$V_f^*=(E_{1t}-E_m)/(E_{ft}-E_m)$$
$$=(3.58-0.0080)/(24.8-0.0080)=0.144$$

Then, using Eq. (C4) for $k=c$:

$$E_{fc}=[E_{1c}-E_m(1-V_f^*)]/V_f^*$$
$$=[0.00120-0.0080(0.856)]/0.144=0.0358 \text{ GPa}$$

From Eq. (C5) with $k = c$,

$$\nu_{fc} = \nu_{12c} / V_f^* = 0.205/0.144 = 1.42$$

Using Eq. (C2), one obtains $\nu_{23c} = 0.202$, whereupon, from Eq. (C1), $G_{23c} = 0.00499$ GPa.

Acknowledgments

The authors are grateful to the Office of Naval Research for financial support through Contract N00014-78-C-0647 and to the University's Merrick Computing Center for providing computing time.

References

[1] Clark, S. K., "The Plane Elastic Characteristics of Cord-Rubber Laminates," *Textile Research Journal*, Vol. 33, April 1963, pp. 295-313.

[2] Zolotukhina, L. I. and Lepetov, V. A., "The Elastic Moduli of Flat Rubber-Fabric Construction in Elongation and Compression," *Soviet Rubber Technology*, Vol. 27, Oct. 1968, pp. 42-44.

[3] Patel, H. P., Turner, J. L., and Walter, J. D., "Radial Tire Cord-Rubber Composites," *Rubber Chemistry and Technology*, Vol. 49, Sept.-Oct. 1976, pp. 1095-1110.

[4] Bert, C. W., "Models for Fibrous Composites with Different Properties in Tension and Compression," *Journal of Engineering Materials and Technology, Transactions of ASME*, Vol. 99H, Oct. 1977, pp. 344-349.

[5] Jones, R. M. and Morgan, H. S., "Bending and Extension of Cross-Ply Laminates with Different Moduli in Tension and Compression," *Proceedings, AIAA/ASME/SAE 17th Structures, Structural Dynamics, and Materials Conference*, King of Prussia, Pa., May 1976, pp. 158-167; *Computers and Structures*, Vol. 11, March 1980, pp. 181-190.

[6] Kincannon, S. K., Bert, C. W., and Sudhakar Reddy, V., "Cross-Ply Elliptic Plates of Bimodulus Material," *Journal of the Structural Division, Proceedings of ASCE*, Vol. 106, No. ST7, July 1980, pp. 1437-1449.

[7] Bert, C. W., Reddy, V. S., and Kincannon, S. K., "Deflection of Thin Rectangular Plates of Cross-Plied Bimodulus Material," *Journal of Structural Mechanics*, Vol. 8, No. 4, 1980, pp. 347-364.

[8] Reddy, J. N., "Finite-Element Analyses of Laminated Composite-Material Plates," School of Aerospace, Mechanical and Nuclear Engineering, Univ. of Oklahoma, Norman, Okla., Contract N00014-78-C-0647, Rept. OU-AMNE-79-9, June 1979.

[9] Shapiro, G. S., "Deformation of Bodies with Different Tensile and Compressive Strengths [Stiffnesses]," *Mechanics of Solids*, Vol. 1, No. 2, 1966, pp. 85-86.

[10] Kamiya, N., "Transverse Shear Effect in a Bimodulus Plate," *Nuclear Engineering and Design*, Vol. 32, July 1975, pp. 351-357.

[11] Whitney, J. M., "The Effect of Transverse Shear Deformation on the Bending of Laminated Plates," *Journal of Composite Materials*, Vol. 3, July 1969, pp. 534-547.

[12] Whitney, J. M. and Pagano, N. J., "Shear Deformation in Heterogeneous Anisotropic Plates," *Journal of Applied Mechanics*, Vol. 37, Dec. 1970, pp. 1031-1036.

[13] Turvey, G. J., "Bending of Laterally Loaded, Simply Supported, Moderately Thick, Antisymmetrically Laminated Rectangular Plates," *Fibre Science and Technology*, Vol. 10, July 1977, pp. 211-232.

[14] Yang, P. C., Norris, C. H., and Stavsky, Y., "Elastic Wave Propagation in Heterogeneous Plates," *International Journal of Solids and Structures*, Vol. 2, Nov. 1966, pp. 665-684.

[15] Mindlin, R. D., "Influence of Rotatory Inertia and Shear on Flexural Motions of Isotropic, Elastic Plates," *Journal of Applied Mechanics*, Vol. 18, March 1951, pp. 31-38.

[16] Wang, A.S.D. and Chou, P. C., "A Comparison of Two Laminated Plate Theories," *Journal of Applied Mechanics*, Vol. 39, June 1972, pp. 611-613.

[17] Hoff, N. J., "Buckling of Axially Compressed Circular Cylindrical Shells at Stresses Smaller than the Classical Critical Value," *Journal of Applied Mechanics*, Vol. 32, Sept. 1965, pp. 542-546.

[18] Reddy, J. N., "A Penalty Plate-Bending Element for the Analysis of Laminated Anisotropic Composite Plates," School of Aerospace, Mechanical and Nuclear Engineering, Univ. of Oklahoma, Norman, Okla., Contract N00014-78-C-0647, Rept. OU-AMNE-79-14, Aug. 1979; also, *International Journal of Numerical Methods in Engineering*, Vol. 15, 1980, pp. 1187-1206.

[19] Reddy, J. N. and Chao, W. C., "Finite-Element Analysis of Laminated Bimodulus Plates," *Computers and Structures*, Vol. 12, 1980, pp. 245-251.

[20] Bert, C. W., Reddy, J. N., Chao, W. C., and Sudhakar Reddy, V., "Vibration of Thick Rectangular Plates of Bimodulus Composite Material," *Journal of Applied Mechanics*, Vol. 48, June 1981, pp. 371-376.

[21] Reddy, J. N., Bert, C. W., Hsu, Y. S., and Sudhakar Reddy, V., "Thermal Bending of Thick Rectangular Plates of Bimodulus Composite Material," *Journal of Mechanical Engineering Science*, Vol. 22, Dec. 1980, pp. 297-304.

[22] Pister, K. S., "Flexural Vibration of Thin Laminated Plates," *Journal of the Acoustical Society of America*, Vol. 31, Feb. 1959, pp. 233-234.

[23] Foye, R. L., "The Transverse Poisson's Ratio of Composites," *Journal of Composite Materials*, Vol. 6, April 1972, pp. 293-295.